

## Nonlinearly Induced $PT$ Transition in Photonic Systems

Yaakov Lumer, Yonatan Plotnik, Mikael C. Rechtsman, and Mordechai Segev

*Physics Department and the Solid State Institute, Technion – Israel Institute of Technology, Haifa 32000, Israel*  
(Received 3 March 2013; published 27 December 2013)

We study the effect of nonlinearity on systems with periodic parity-time ( $PT$ ) symmetry, and show that nonlinearity can transform the system from broken to full  $PT$  symmetry and vice versa. Furthermore, we show that even when the nonlinearity is insufficient to induce a transition from broken to full  $PT$  symmetry, still, the wave functions neither decay nor diverge, despite the fact that the system has a complex eigenvalue spectrum. Rather, the amplitudes of the wavefunctions oscillate around the transition point. Our results apply to a wide variety of systems in optics and beyond.

DOI: [10.1103/PhysRevLett.111.263901](https://doi.org/10.1103/PhysRevLett.111.263901)

PACS numbers: 42.65.Sf, 42.65.Wi

For decades, it was believed that physical phenomena in quantum systems must be described by Hermitian Hamiltonians, since it was thought that only they always have real eigenvalues. However, in 1998 it was shown that non-Hermitian systems obeying parity-time symmetry ( $PT$ ) can have real spectra, despite a complex potential [1,2]. While an experimental realization of such quantum systems has yet to be demonstrated, in optics  $PT$  symmetry is realizable, with the complex potential arising from optical gain and loss. Indeed,  $PT$ -symmetric optical potentials were proposed with two coupled waveguides [3,4], one with gain and the other with an identical amount of loss. Experimental demonstrations of  $PT$ -symmetric optical systems were pioneered by using passive elements [5], by inducing gain or loss via photorefractive two-wave mixing [6], and, recently, in a temporal photonic  $PT$ -symmetric lattice [7]. The concepts of  $PT$  symmetry were also extended to electrical circuits [8,9], observing nonreciprocal behavior [8] and using  $PT$  symmetry to bypass the bandwidth theorem [9]. Subsequently, periodicity was introduced, making  $PT$ -symmetric lattices and adding new phenomena [10–12], such as double refraction, asymmetric diffraction, and unidirectional invisibility [13]. Likewise, adding nonlinearity was predicted to support novel phenomena, such as solitons in  $PT$  structures [13–17].

One of the key features of any  $PT$ -symmetric system is the transition of the eigenvalue spectrum from being real to complex. Whether the spectrum is real or not is determined by a single parameter: the magnitude of the imaginary part of the potential relative to the real part. When that parameter is below a specific threshold, the spectrum is completely real, and the system is fully  $PT$  symmetric. When that parameter is above that threshold, the spectrum has complex eigenvalues, and the system has broken  $PT$  symmetry. At the transition, the system has exceptional points [4], at which two eigenvectors coalesce, becoming self-orthogonal [18–21]. Clearly, nonlinearity can have a major impact on the  $PT$ -symmetry of a system, because it can change the ratio between the real and imaginary parts of the

susceptibility. Thus far, nonlinear  $PT$ -symmetric systems were explored in the context of solitons [14–17,22,23], breathers [24], and stable nonlinear modes in few-waveguide systems [25]. However, the  $PT$ -symmetry-breaking transition has always been set by the linear part, while the effects of nonlinearity on the  $PT$  transition have not been studied.

Here, we show that the  $PT$  transition can be induced or suppressed by introducing nonlinearity. We show that, for a linear system with broken  $PT$  symmetry, it is possible to induce the  $PT$  transition into a completely real spectrum of nonlinear eigenmodes by increasing nonlinearity, or the opposite—from full to broken  $PT$  symmetry by increasing nonlinearity of the opposite sign. In addition, in the regime of broken- $PT$  symmetry with insufficient nonlinearity to induce the transition, we observe periodic oscillatory dynamics with the peak power neither diverging nor decaying, despite the fact that the linear system has a complex spectrum. This oscillatory dynamics is related to the nonlinear  $PT$  phase transition in the band structure. These findings pave the way to nonlinear control over the  $PT$  transition and associated phenomena: exceptional points, divergence of their associated wave functions, unidirectional power flow, etc. [4,13,20,26].

We begin with a linear description of our system, using the (1 + 1)D paraxial wave equation, in dimensionless units:

$$i\partial_z\psi + \partial_x^2\psi + V(x)\psi = 0, \quad (1)$$

where  $\psi$  is the wave function,  $z$  is the spatial coordinate along the propagation axis,  $x$  is the transverse coordinate, and  $V(x)$  corresponds to the refractive index change. Importantly, Eq. (1) is equivalent to the Schrödinger equation [27]; thus, the subsequent results are applicable to any system obeying Schrödinger dynamics. For the system to be  $PT$  symmetric,  $V(x)$  must be symmetric to successive action of the parity ( $P$ ) and time-reversal ( $T$ ) operators:  $PT\{V(x)\} = V^*(-x) = V(x)$ , while  $V(x)$  need not obey  $P$  or  $T$ , separately. Here, we use a periodic potential with period  $D = \pi$  [11]:

$$V(x) = 4(\cos^2(x) + iV_0 \sin(2x)), \quad (2)$$

where  $V_0$  is the strength of the imaginary part of the potential relative to its real part [Fig. 1(a)]. Because the potential is periodic, its eigenfunctions obey Bloch periodicity: they are of the form  $\varphi(x) = u(x)e^{ikx}$ , where  $u(x)$  is  $D$  periodic, and  $k$  is the Bloch wave number. As an example, the intensity pattern of the first two modes with  $k = 0.87 \pi/D$  and  $V_0 = 0.52$  is shown in Fig. 1(b). Calculating the energy spectrum of the potential in Eq. (2), one can see that the eigenvalues (energies) are strictly real for  $V_0 \leq 0.5$  [14], while for  $V_0 > 0.5$  some are complex. In this latter case, the system has broken  $PT$  symmetry despite the fact  $V(x)$  obeys the  $PT$ -symmetry prerequisites (symmetric  $\text{Re}[V(x)]$  and antisymmetric  $\text{Im}[V(x)]$ ). Such a complex spectrum is shown in Fig. 1(c) for  $V_0 = 0.52$  (first two bands). Notice that, while the center of the Brillouin zone contains purely real energies, at the edges [ $k = \pm(\pi/D)$ ] the energies are complex. Figures 1(d) and 1(e) show the Brillouin zone edge, centered at  $k = \pi/D$ . The size of the region with complex energies increases as  $V_0$  increases. This effect is most pronounced in the first two bands [Figs. 1(d) and 1(e)], although the transition can occur simultaneously in all bands [16].

Next, we show that adding nonlinearity can induce a transition from broken to full  $PT$  symmetry. Adding Kerr nonlinearity, our system is described by

$$i\partial_z \psi + \partial_x^2 \psi + V(x)\psi + n_2 |\psi|^2 \psi = 0, \quad (3)$$

where  $n_2$  is the sign of the nonlinearity— $n_2 = 1$  ( $n_2 = -1$ ) for focusing (defocusing) nonlinearity, respectively. In these units, the magnitude of the nonlinear effects is

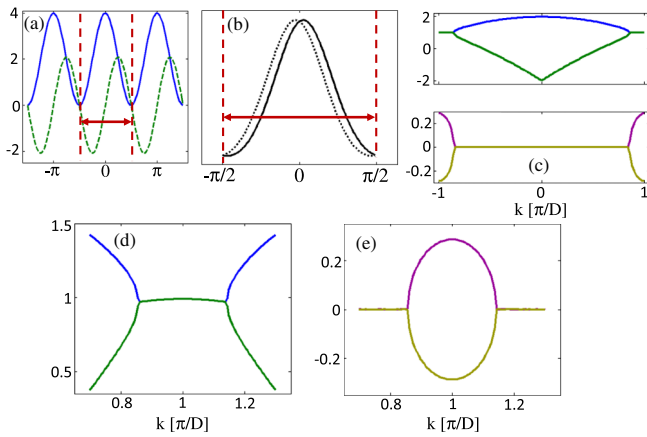


FIG. 1 (color online). (a) Real (solid blue) and imaginary (dashed green) parts of the periodic potential  $V(x)$ . (b) Intensity wave functions of the first two guided modes for  $k = 0.87$ . Solid: mode with gain. Dashed: mode with loss. The arrow between the dashed vertical lines indicates the unit cell of  $V(x)$ , highlighting the spatial scale. (c) Real (top) and imaginary (bottom) parts of the eigenvalue spectrum of  $V(x)$ . (d), (e) The spectrum shown in (c), centered at the Brillouin zone edge  $k = \pi/D$ .

manifested in the amplitude of  $\psi$ . We calculate the nonlinear band structure: the extended eigenmode solutions to the nonlinear eigenvalue problem, obeying Bloch periodicity. Thus, we solve

$$\beta \psi = \partial_x^2 \psi + V(x)\psi + n_2 |\psi|^2 \psi, \quad (4)$$

with  $\psi(x) = u(x)e^{ikx}$ , where  $u(x)$  is  $D$  periodic,  $k$  is the Bloch wave number, and  $\beta$  is the energy. We define the power contained in the wave function in a single unit cell as  $P = \int_{\text{unit cell}} |\psi|^2 dx$ , and solve Eq. (4) for all  $k$ 's for each  $P$ . Here,  $P$  is a measure of the strength of the nonlinearity. We employ the self-consistency method for the calculation of the nonlinear extended states [28,29]. The nonlinear spectra for focusing nonlinearity ( $n_2 = 1$ ) for  $P$  varying from 0.3 to 0.5 are shown in Figs. 2(a)–2(h). Notice that, for  $P = 0.3$  [Figs. 2(a) and 2(b)] the spectrum looks qualitatively the same as the linear one [Fig. 1(c)]; however, the size of the region with complex energies is smaller, and the maximal imaginary energy is also smaller. As we increase

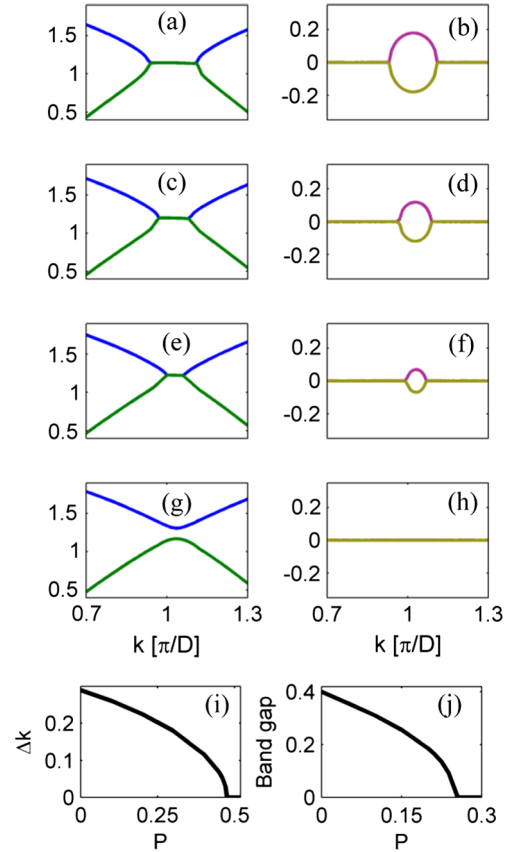


FIG. 2 (color online). (a)–(h) Real (left column) and imaginary (right column) parts of the nonlinear spectrum with nonlinearity of the focusing type  $n_2 = 1$  and  $V_0 = 0.52$ . (a), (b)  $P = 0.3$ , (c), (d)  $P = 0.4$ , (e), (f)  $P = 0.45$ , and (g), (h)  $P = 0.5$ . (i) Size of the complex region of the spectrum  $\Delta k$  vs the power  $P$  for potential  $V(x)$  with  $V_0 = 0.52$ . (j) Gap of real spectrum for potential  $V(x)$  with  $V_0 = 0.49$  vs the power  $P$  with nonlinearity of the defocusing type  $n_2 = -1$ .

$P$ , this trend continues, and the region in the Brillouin zone where the energies are complex becomes smaller. The variation of the size of the complex region of the spectrum as the power  $P$  is increased is summarized in Fig. 2(i). For  $P > 0.5$ , the region where the energies are complex has disappeared, and the whole spectrum is now real. Clearly, the nonlinearity has induced a  $PT$  transition from broken  $PT$  symmetry to a fully  $PT$ -symmetric state, with a real spectrum. The opposite is also true: nonlinearity can break the  $PT$  symmetry of a system. In this case, the nonlinearity is of the defocusing type ( $n_2 = -1$ ). To show this, we begin with a linear system that is  $PT$  symmetric with  $V_0 = 0.49$ . The system has a real spectrum, with a gap between the first and second bands. As we increase  $P$ , the gap narrows, until it closes and complex eigenvalues emerge [Fig. 2(j)].

Next, we study the nonlinear dynamics of a wave packet near the transition point, specifically the dynamics of the transition from a complex to a real spectrum, for the focusing case. In order to avoid modulation instability in our simulations [28], we do this by propagating extended waves with a well-defined Bloch wavenumber  $k$ . Such a restriction does not allow perturbations of spatial wavelength longer than  $1/k$  to be amplified, suppressing modulation instability. To see the nonlinear transition, we need to choose  $k$  such that the linear system has a complex eigenvalue at that  $k$ . For a large enough nonlinearity, the eigenvalues corresponding to that particular  $k$  are real. We choose  $k = 0.87 \pi/D$ . First, we launch an eigenstate of the nonlinear system that has a real eigenvalue, with power  $P = 0.3$ . The results of the numerical propagation simulation of that eigenstate are shown in Figs. 3(a) and 3(b), where it is evident that the intensity [Fig. 3(a)] and power

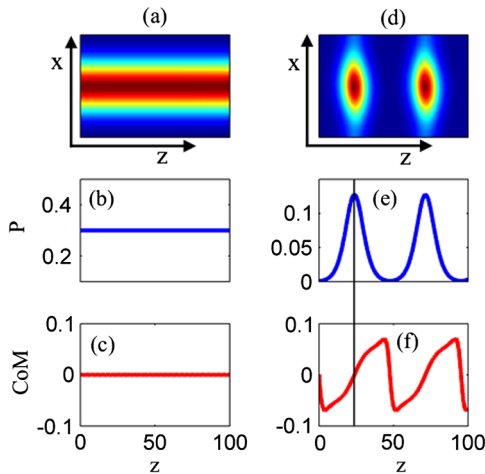


FIG. 3 (color online). (a),(b),(c) Evolution of the intensity, total power, and position of the "center of mass" of the nonlinear eigenstate during propagation, for power levels that transform the system from broken to full  $PT$  symmetry. (d),(e),(f) Same as (a)–(c) for the wave with low initial power that does not induce the  $PT$  transition.

[Fig. 3(b)] are invariant throughout propagation. This proves that indeed when the nonlinearity has induced the transition from broken to full  $PT$  symmetry, the propagation dynamics is stationary as expected, as the eigenvalues have become real. Let us now examine what happens when we launch the same wave but with very low power,  $P = 0.001$ , which is far too low to induce the transition. The propagation dynamics of such a nonlinear mode is shown in Figs. 3(d) and 3(e). Because the power is very low, the nonlinearity has a negligible effect and the propagation at the beginning is linear. Since the system has broken  $PT$  symmetry, the eigenvalues are complex and the wave gains power. The power increases until it passes the power level at which the nonlinear eigenvalues are real. The power continues to increase, until it reaches a certain maximum value and then it starts to *decrease* until the power becomes very low again. Then the dynamics is linear again, and the cycle starts over. These dynamics are shown in Figs. 3(d) and 3(e). Such oscillatory dynamics continue for very long distances.

It is important to study the stability of the nonlinear modes in the regime where the nonlinearity has induced full  $PT$  symmetry, and also of the nonlinear oscillatory modes. Linear stability analysis reveals that all the modes in the nonlinearly induced full  $PT$  symmetry [e.g., Figs. 3(a) and 3(b)] are stable, and these modes are characterized by a real propagation constant (even though in the linear system they reside in the broken  $PT$ -symmetry regime) [30]. In fact, we find that the dynamics of perturbations around these eigenmodes is also  $PT$  symmetric [30]. In the nonlinear oscillatory regime [e.g., Figs. 3(d) and 3(e)], propagation simulations indicate that stable oscillatory dynamics should continue indefinitely.

The nonlinear oscillatory dynamics can be explained by examining the motion of the center-of-mass (c.m.) during propagation [Fig. 3(f)]. The evolution starts at the center of the unit cell. Because its initial power is low, we can decompose it into the two linear complex eigenmodes: one with eigenvalue with a positive imaginary part (gain) and one with a negative imaginary part (loss). Naturally, the eigenstate with gain resides mostly in the gain half of the potential [c.m.  $< 0$  in Fig. 3(f)], while the lossy eigenstate resides mostly in the loss half [c.m.  $> 0$  in Fig. 3(f)]. Thus, following the linear propagation, the lossy eigenstate quickly dies out and only the gain eigenstate survives, which shifts the c.m. downwards. When the power continues to increase, the system passes the nonlinear transition point and the system becomes  $PT$  symmetric; hence, all of its nonlinear eigenvalues become real [31]. Thus, a "gain eigenmode" no longer exists, and the wave packet is attracted to the center of the unit cell, where the potential is deepest. However, when it reaches the center, it has upwards momentum, which drives it into the lossy region. There, the power decreases until it reaches levels where the nonlinearity is insignificant and the system again has

complex eigenvalues. Thus, the wave is again attracted to the gain region, and the entire dynamics continues periodically. This nonlinear oscillatory dynamics resembles that of a harmonic oscillator, albeit a non-ideal one since the c.m. oscillations are not strictly sinusoidal. The nonlinear oscillations shown in Figs. 3(d)–3(f), which always occur when the initial state has low power and broken  $PT$  symmetry, seem to resemble the behavior of the breathers found when the system is fully  $PT$  symmetric [24]. However, the differences between the two phenomena are profound. Namely, the nonlinear breathers arise from interference between nonlinear modes occurring strictly in the full  $PT$ -symmetric regime, as their eigenvalues are real, whereas the nonlinear oscillations shown in Fig. 3 arise from crossing back and forth across the  $PT$ -transition point.

Finally, we compare the maximum power in the dynamic simulations for a specific  $k$ , to the power at which the eigenvalues at that  $k$  become real. We expect these two values to be strongly correlated, since both reflect the nonlinear  $PT$  transition. In Fig. 4(a), the solid curve represents the maximal power in dynamic simulations (for initially weak power) vs  $k$ , and the dotted curve is the power at which the spectrum at each  $k$  becomes real. Both curves follow the same trend, although they do not coincide. This follows from the fact that the oscillatory dynamics causes the power to "overshoot" the  $PT$ -transition point. However, if we multiply the dynamic maximum power by factor of 0.5, we get an excellent match between the two curves [Fig. 4(b)]. This proves that the dynamic evolution is dictated by the nonlinear  $PT$  transition. The factor of 0.5 is not universal, namely, it is potential dependent. For potentials that follow Eq. (2), the factor 0.5 is consistent for all values of  $V_0$ . However, if we compare the dynamic  $PT$  transition to the  $PT$  transition in the Bloch spectrum for a different potential structure, for example, a rectangular-shaped lattice, we get an exact match like Fig. 4(b), but with a factor of 0.63.

Analysis of the results shows that, for the nonlinear  $PT$  transition to occur, the wave functions of the two modes of

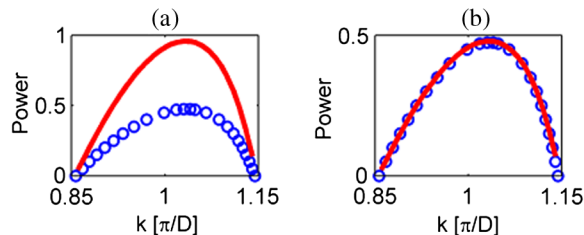


FIG. 4 (color online). Comparison of the ratio between the maximum power in the dynamic simulations for a specific  $k$ , to the power level at which the eigenvalues at that specific  $k$  become real. (a) Simulated evolution of the maximal power. Blue circles: power level at which the eigenvalues at that specific  $k$  become real. (b) Same as (a) but with red curve multiplied by a factor of 0.5.

the broken  $PT$  system (the mode in the gain region and the mode in the loss region) must have a strong spatial overlap, as is the case in the potential analyzed here. In such cases, the nonlinearity strongly affects the modes and the coupling between them. A nonlinear  $PT$  transition cannot happen in systems where the modes are spatially separated. This brings an important insight: a nonlinear  $PT$  transition does not occur in systems modeled by a standard tight-binding (coupled-mode) model with an on-site nonlinearity, such as the discrete nonlinear Schrödinger equation with an on-site cubic term and alternating gain and loss [25]. In such a system, the nonlinearity affects the on-site energy only, but inherently cannot capture the effects of nonlinear coupling between the modes guided in the gain and the loss regions, which is required for the nonlinear  $PT$  transition. Instead, the effects of nonlinearity in such a system are completely different [25]: while it can cause the emergence of modes with real energies, it cannot transform complex energies into real ones. In fact, in such cases the nonlinearity can even cause modes with real energies to bifurcate into modes that have complex energies, breaking the  $PT$  symmetry [32]. In sharp contrast, in systems with strong spatial overlap between the modes, the nonlinearity can transform the “complex modes” into “real modes” which maintain their shape and amplitude throughout propagation. We emphasize that this spatial modal overlap (required for having a nonlinear  $PT$  transition) occurs naturally in *any* continuous physical system. The standard tight-binding model with on-site nonlinearity fails to describe such effects, but one can extend tight binding to include effects of nonlinearity in the coupling coefficients [30]. In such a case, the nonlinear  $PT$  transition can be observed even using simple models [30].

Before closing, we examine the impact of modulation instability on the nonlinear dynamics. We employ simulations of the full lattice (not just in a single unit cell, as in Fig. 3), such that we capture also the very low (transverse) wave number modulation occurring on scales of multiple unit cells. The results are presented in [30]. We find that, up to 1% noise, the single unit cell oscillations presented in Fig. 3 represent the true dynamics in the system up to several nonlinear oscillations. Eventually, modulation instability prevails, but before this occurs the nonlinear dynamics is dominated by the oscillations shown in Fig. 3 [30].

In conclusion, we have shown that in systems obeying  $PT$  symmetry, nonlinearity can overcome broken symmetry, transforming a linear system that has complex eigenvalues into a nonlinear one with strictly real eigenvalues (and vice versa). We described this transition by calculating the nonlinear Bloch spectrum for a periodic system, showing that as we increase the strength of the nonlinearity, the imaginary part of the complex eigenvalues decreases until it vanishes. In addition, we simulated the nonlinear dynamics of waves in the broken  $PT$ -symmetry



regime and whose power is insufficient to induce the transition to full  $PT$  symmetry. We find these nonlinear waves to exhibit oscillations in their power and intensity structure. Altogether, the nonlinear  $PT$  transition presented here happens in systems with strong overlap between the spatial modes associated with the gain and loss regions, and, consequently, the nonlinearity strongly affects the coupling between these modes. The importance of this nonlinear  $PT$  transition, among other things, is in the ability to design systems that can switch from being power conservative to systems with gain, by changing the power of the wave alone. Future work will explore higher dimensions, other potentials allowing for nonlinear  $PT$  transition, and experimental realizations of a nonlinear  $PT$  system where the transition from broken to full  $PT$  symmetry is induced through by the wave itself.

This work was supported by the Israeli Center of Research Excellence (I-CORE) ‘Circle of Light’, by the Israel Science Foundation, by the Binational USA-Israel Science Foundation (BSF), and by an Advanced Grant from the European Research Council.

- 
- [1] C. M. Bender and S. Boettcher, *Phys. Rev. Lett.* **80**, 5243 (1998).
- [2] C. M. Bender, D. C. Brody, and H. F. Jones, *Phys. Rev. Lett.* **89**, 270401 (2002).
- [3] R. El-Ganainy, K. G. Makris, D. N. Christodoulides, and Z. H. Musslimani, *Opt. Lett.* **32**, 2632 (2007).
- [4] S. Klaiman, U. Günther, and N. Moiseyev, *Phys. Rev. Lett.* **101**, 080402 (2008).
- [5] A. Guo, G. J. Salamo, D. Duchesne, R. Morandotti, M. Volatier-Ravat, V. Aimez, G. A. Siviloglou, and D. N. Christodoulides, *Phys. Rev. Lett.* **103**, 093902 (2009).
- [6] C. E. Rüter, K. G. Makris, R. El-Ganainy, D. N. Christodoulides, M. Segev, and D. Kip, *Nat. Phys.* **6**, 192 (2010).
- [7] A. Regensburger, C. Bersch, M.-A. Miri, G. Onishchukov, D. N. Christodoulides, and U. Peschel, *Nature (London)* **488**, 167 (2012).
- [8] Z. Lin, J. Schindler, F. M. Ellis, and T. Kottos, *Phys. Rev. A* **85**, 050101(R) (2012).
- [9] H. Ramezani, J. Schindler, F. M. Ellis, U. Gunther, and T. Kottos, *Phys. Rev. A* **85**, 062122 (2012).
- [10] K. G. Makris, R. El-Ganainy, D. N. Christodoulides, and Z. H. Musslimani, *Phys. Rev. Lett.* **100**, 103904 (2008).
- [11] K. G. Makris, R. El-Ganainy, D. N. Christodoulides, and Z. H. Musslimani, *Phys. Rev. A* **81**, 063807 (2010).
- [12] A. Szameit, M. C. Rechtsman, O. Bahat-Treidel, and M. Segev, *Phys. Rev. A* **84**, 021806(R) (2011).
- [13] H. Ramezani, T. Kottos, R. El-Ganainy, and D. N. Christodoulides, *Phys. Rev. A* **82**, 043803 (2010).
- [14] Z. H. Musslimani, K. G. Makris, R. El-Ganainy, and D. N. Christodoulides, *Phys. Rev. Lett.* **100**, 030402 (2008).
- [15] S. Suchkov, B. A. Malomed, S. V. Dmitriev, and Y. S. Kivshar, *Phys. Rev. E* **84**, 046609 (2011).
- [16] S. Nixon, L. Ge, and J. Yang, *Phys. Rev. A* **85**, 023822 (2012).
- [17] V. Achilleos, P. G. Kevrekidis, D. J. Frantzeskakis, and R. Carretero-Gonzalez, *Phys. Rev. A* **86**, 013808 (2012).
- [18] N. Moiseyev and S. Freidland, *Phys. Rev. A* **22**, 618 (1980).
- [19] O. Peleg, M. Segev, G. Bartal, D. N. Christodoulides, and N. Moiseyev, *Phys. Rev. Lett.* **102**, 163902 (2009).
- [20] B. Alfassi, O. Peleg, N. Moiseyev, and M. Segev, *Phys. Rev. Lett.* **106**, 073901 (2011).
- [21] Y. D. Chong, L. Ge, and A. D. Stone, *Phys. Rev. Lett.* **106**, 093902 (2011).
- [22] F. K. Abdullaev, Y. V. Kartashov, V. V. Konotop, and D. A. Zezyulin, *Phys. Rev. A* **83**, 041805(R) (2011).
- [23] M.-A. Miri, A. B. Aceves, T. Kottos, V. Kovanis, and D. N. Christodoulides, *Phys. Rev. A* **86**, 033801 (2012).
- [24] I. V. Barashenkov, S. V. Suchkov, A. A. Sukhorukov, S. V. Dmitriev, and Y. S. Kivshar, *Phys. Rev. A* **86**, 053809 (2012).
- [25] D. A. Zezyulin and V. V. Konotop, *Phys. Rev. Lett.* **108**, 213906 (2012).
- [26] A. A. Sukhorukov, Z. Xu, and Y. S. Kivshar, *Phys. Rev. A* **82**, 043818 (2010).
- [27] S. Longhi, *Laser Photon. Rev.* **3**, 243 (2009).
- [28] O. Cohen, T. Schwartz, J. E. Fleischer, M. Segev, and D. N. Christodoulides, *Phys. Rev. Lett.* **91**, 113901 (2003); H. Buljan, O. Cohen, J. W. Fleischer, T. Schwartz, M. Segev, Z. H. Musslimani, N. K. Efremidis, and D. N. Christodoulides, *Phys. Rev. Lett.* **92**, 223901 (2004); M. Jablan, H. Buljan, O. Manela, G. Bartal, and M. Segev, *Opt. Express* **15**, 4623 (2007).
- [29] If  $\beta$  is complex, the nonlinear mode is not really shape preserving, as its power is increasing or decreasing during propagation, thus changing the nonlinear potential it induces.
- [30] See Supplemental Material at <http://link.aps.org/supplemental/10.1103/PhysRevLett.111.263901> for details.
- [31] We refer to these nonlinear eigenfunctions as “modes” even though generally superposition does not hold in a nonintegrable system as ours. However, the nonlinear dynamics in this system (e.g., Fig. 3) can be heuristically explained through these modes and it yields surprisingly accurate insight.
- [32] This is what happens, for example, in [25], as careful modal analysis reveals for the case of Fig. 1 therein.